International Journal of Science and Engineering Applications
Volume 11-Issue 12, 254 – 265, 2022, ISSN:- 2319 - 7560
DOI: 10.7753/IJSEA1112.1002

Calculation of the Single-Walled Carbon Nanotubes' Elastic Modulus by Using the Asymptotic Homogenization Method

Sima Besharat Ferdosi
Department of Mechanical Engineering,
Lamar University,
Beaumont, TX, US

Meisam Porbashiri
Department of Mechanical Engineering,
Ferdowsi University,
Mashhad, Iran

Abstract: This article uses the asymptotic homogenization method to investigate the mechanical characteristics of single-walled carbon nanotubes. The asymptotic homogenization method has been used to derive the equations for the homogenized elastic properties matrix. Then, MATLAB is used to model nanotubes and implement the finite element simulation. Two types of chiralities, including armchair and zigzag, are taken into account in this regard. Young's modulus and shear modulus have been estimated for both armchair and zigzag nanotubes in accordance with the relationships between the derived coefficients and molecular mechanical characteristics. Investigations have been done into how diameter and orientation affect the mechanical characteristics of carbon nanotubes. The research's findings are corroborated and generally consistent with those found in other articles.

Keywords: Carbon nanotubes, Asymptotic homogenization, Periodic systems, Homogenized elastic property matrix, Young's modulus, Shear modulus.

1. INTRODUCTION

Today, with the progress of science, there are need to produce smaller parts in various industries such as the military, aviation, electronics, etc. Assembling these requires in order to the production of advanced materials with higher efficiency, leading to the increasing progress of research in the field of nanotechnology. Carbon nanotubes have a special importance in the field of nanotechnology due to their unique properties that they have, which led various scientists and researchers to try to accurately predict their properties. Kroto et al [1] investigated the mechanism of the carbon molecular chain and introduced fluorine by laser irradiation on the surface of graphite. During this approach, a significant group of 60 carbon atoms with 5 and 6-sided arrangements are formed in the form of a closed shelf that is arranged in the form of a soccer ball. A few years after the discovery of fullerenes, carbon nanotubes were accidentally discovered in 1991 by Sumio Iijima [2] while studying carbon electrodes during electronic discharge.

Carbon nanotubes have remarkable mechanical, thermal, and electrical properties due to their symmetrical structure. They are mechanically classified in the hard materials classes. In equal weight with the hard steel, they are expected to show resistance more than about one hundred times. In terms of thermal properties, nanotubes are stable up to 2800 degrees Celsius in a vacuum and up to 750 degrees Celsius in air. Moreover, they have two times higher thermal conductivity than pure diamonds. Also, in comparison with copper, carbon nanotubes have 100 times more electrical load-carrying capacity [3]. In addition, carbon nanotubes can behave as conductive or semi-conductive, which is due to the arrangement of carbon atoms [4]. Due to the unique mechanical properties of carbon nanotubes, extensive studies and research have been conducted in this field, and these studies can be divided into two experimental and theoretical parts.

Krishman et al [5] experimentally tested 27 single-walled nanotubes in the diameter range of 1-1.5 nm using thermal vibration analysis and obtained Young's modulus of 0.9 to 1.7 TPa. By using an atomic force microscope, Tumbler et al. [6] obtained Young's modulus of about 1.2 TPa. Salvetat et al. [7] also found a value of 0.8 to 1.2 TPa for Young's modulus of carbon nanotubes utilizing an atomic force microscope. During theoretical research, Hernandez et al. [8] using the non-orthogonal tight junction formulation and considering the wall thickness as 0.34 nm, obtained Young's modulus of approximately 1.22 to 1.24 TPa for single-walled nanotubes.

Arroy et al. [9] approximated Young's modulus 0.686 TPa by using large atomic deformations based on the Tersoff-Brenner potential function. Li and Chou [10] modeled the deformation of carbon nanotubes using structural mechanics approximation and stiffness matrix method and obtained Young's modulus equal to 0.89 -1.3 TPa and shear modulus equal to 0.27-0.49 TPa. Also, using the aforementioned method, they illustrated that the mechanical behavior of armchair and zigzag nanotubes is dependent on the diameter and orientation of the nanotube. Jin and Yuan [11] used the molecular dynamics method to investigate the mechanical properties of carbon nanotubes. By acquisition of numerical methods and using two

approximations of energy and force, they obtained the mechanical properties of nanotubes with a diameter range of 0.407 to 1.357 nm. By using the energy method, Young's modulus and the shear modulus were equal to 1.236 TPa and 0.49 TPa respectively. Simultaneously, by using the force method, Young's modulus was obtained equal to 1.35 TPa, and the shear modulus was calculated 0.45 TPa. Tserpes and Papanikos [12] by hiring the structural mechanic's method and using 3D finite elements, modeled armchair, zigzag, and chiral nanotubes. They investigated the effect of three factors nanotubes consist of wall thickness, nanotube diameter, and orientation on the mechanical properties of nanotubes. Their investigations demonstrated that the mechanical properties of nanotubes are highly sensitive to changes in thickness, diameter, and orientation. For the wall thickness of 0.34 nm, the gained results from their method predicted Young's modulus of about 0.952 to 1.066 TPa and the shear modulus of approximately 0.242 to 0.504 TPa.

Xiao et al. [13] investigated the mechanical properties of nanotubes using the analytical molecular structure mechanics approach and using the modified Morse potential function. Their model was able to predict Poisson's ratio, Young's modulus, and the stress-strain relationship of nanotubes under tensile and shear loading. They showed that Young's modulus of the nanotube is sensitive to the change in diameter and orientation as well. They achieved Young's modulus between 1 to 1.2 TPa, and shear modulus between 0.4 to 0.46 TPa. They also gained the Poisson's ratio between 0.2 and 0.35. Kalamkarov et al. [14], with the homogenization method, obtained Young's modulus and shear modulus equal to 1.717 TPa and 0.322 TPa respectively. Chandraseker and Mukherjee [15] calculated the elastic modulus and stress-strain curve of nanotubes using the *ab initio* approximation and the atomic continuum approximation. They hired the experimental interatomic potential, Christoph-Brenner in the atomic continuum approximation. The obtained results stated that the mechanical properties of the nanotube do not depend on the diameter and orientation, Young's modulus is between 0.47-0.69 TPa and the shear modulus is between 0.19-0.24 TPa. Rafiee et al. [16] predicted Young's modulus of carbon nanotubes using the complete nonlinear finite element model. They benefited the spring element to approximate molecular interactions in the atomic structure of nanotubes. Considering the nonlinear effects, they found that Young's modulus of the nanotube is independent of the orientation and diameter of the nanotube, and they obtained Young's modulus of about 1.325 TPa for the single-walled nanotube.

2. THE MOLECULAR STRUCTURE OF SWCNTS

A hexagonal lattice of graphene is rolled up into a round-hollow tube to make single-walled carbon nanotubes, Figure (1). The geometrical structure of the arrangement of atoms in carbon nanotubes is defined as chirality which is characterized by the chiral vector *Ch* and the chiral angle θ. The orientation vector *Ch* can be defined as a linear combination of unit basis vectors in the hexagonal lattice as follows:

$$Ch = na_1 + ma_2 \quad (1)$$

In Eq. (1), a chiral angle denotes the direction of the chiral vector θ:

$$\theta = \cos^{-1}\frac{(2n+m)}{2\sqrt{((n^2+m^2+nm)}} \quad (2)$$

The chiral angles are 30° and 0°, when $n = m$ and $n = 0$, are respectively substituted for armchair and zigzag nanotubes. However, the radius of nanotubes at room temperature can be calculated as follows:

$$R = \frac{length\ of\ Ch}{2\pi} = \frac{a\sqrt{(n^2+m^2+nm)}}{2\pi} \quad (3)$$

The equilibrium bond length of the atoms in the graphite sheets is denoted by the expression $a = a_0\sqrt{3}$ [5]

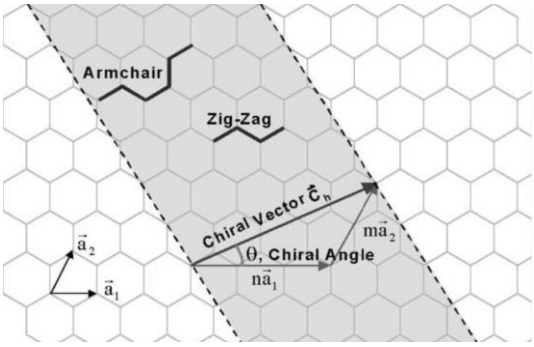

Figure 1. Armichair and zigzag nanotubes developed from graphene [19]

Chirality has a significant effect on the properties of nanotubes, including electrical conductivity, mechanical strength, and optical properties. Unlike graphite, which is considered a semiconductor, nanotubes can behave as a metal or a semi-metal according to the orientation vector [20].

3. ASYMPTOTIC HOMOGENIZATION METHOD

With recent technological advancements, the utilization of composite materials in the industry has grown significantly. Composite materials are materials with distinct constituents whose qualities differ from the constituents themselves. Solids and voids are included in the classification of cellular bodies as a simple type of composite. It is possible to think of a composite with regular heterogeneity as having an alternating or periodic structure. It should be highlighted that this heterogeneity's

International Journal of Science and Engineering Applications
Volume 11-Issue 12, 254 – 265, 2022, ISSN:- 2319 - 7560
DOI: 10.7753/IJSEA1112.1002

size should be extremely small in relation to the object's dimensions. These composites might be referred to as periodic microstructures based on modeling assumptions. The study of boundary value problems, including a significant amount of inhomogeneity, is highly challenging even with the aid of contemporary, high-speed computers. The natural solution to this issue is to substitute the composite with an equivalent model, a process known as homogenization [21]. The mechanical properties of the corresponding homogenized model were calculated using the theory of homogenization, which was created in 1970 [22–24]. In order to acquire the properties of the material on this scale, the first step in the homogenization theory is to mathematically assume that the material structure is periodic and solve the issues on the unit cell. The boundary value problems for the entire material come next in the second step.

4. PERIODICITY AND ASYMPTOTIC EXPANSION

An inhomogeneous material has a regular periodic structure if the functions defining the physical quantities or geometry of the material obey the following property.

$$F\left(x+NY\right) = F(\mathrm{x}) \tag{4}$$

$\mathbf{x} = [\mathbf{x_1}, \mathbf{x_2}, \mathbf{x_3}]^{\mathbf{T}}$ is the position vector of points and N is a 3x3 matrix as follows:

$$N=\begin{bmatrix} n_1 & 0 & 0 \\ 0 & n_2 & 0 \\ 0 & 0 & n_3 \end{bmatrix} \tag{5}$$

In Eq. (4), $\mathbf{Y} = (\mathbf{Y_1}, \mathbf{Y_2}, \mathbf{Y_3})$ is a constant vector that determines the periodicity of the structure, and *F* can be a scalar, a vector, or even a tensor function of the location vector **X**. In a composite material with periodic repetition of **Y** unit cells, the mechanical behavior is described by the following relation:

$$\sigma_{ij} = C_{ijkl}\, e_{kl} \tag{6}$$

The $\boldsymbol{C_{ijkl}}$ tensor is a periodic function of the spatial coordinate **X**. Therefore, the following equation is obtained:

$$C_{ijkl}\left(x+NY\right) = C_{ijkl}\left(x\right) \tag{7}$$

$\boldsymbol{C_{ijkl}}$ has a periodicity of **Y**. In the theory of homogenization, it is assumed that period **Y** is small compared to the dimensions of the problem. In general, we will encounter two behaviors in a composite with a periodic structure. The first one is at the macroscopic level or the global level of **X**, which shows slow changes, and the other is at the microscopic level or the local level of y, which describes fast fluctuations. The ratio of the actual length of a single vector in microscopic coordinates to the actual length of a vector in macroscopic coordinates is defined by the parameter ε as follows:

$$Y = (\frac{x}{\varepsilon}) \tag{8}$$

The functions that determine the behavior of composites can be expressed as follows:

$$Q^{\varepsilon}\left(x\right) = Q^{0}\left(x,y\right) + \varepsilon Q^{1}\left(x,y\right) + \varepsilon^{2}Q^{2}\left(x,y\right) + \ldots \tag{9}$$

This method is called *Double asymptotic expansion*. This extension means that the approximate function of **X** and **Y** converges to the original function at infinity [21].

5. ELASTICITY IN CELLULAR BODIES

This section explains the homogenization approach for cellular materials in the weak form state and extracts the essential equations for a numerical solution using finite elements. Guedes and Kikuchi were the first to employ this technique [25].

When volume force *f* and traction vector *t* are applied to a porous and pore-filled material with alternating microstructures, the elastic problem is taken into account.

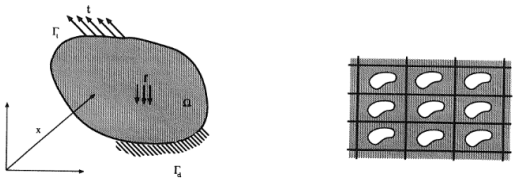

Figure 2. The problem of elasticity in a cellular body [26].

Ω is the range of R3 space with smooth boundaries Γ including Γ*d* (displacement boundaries) and Γ*t* (traction boundaries).

The main cell of the **Y** cell body is shown in figure (3). The domain **Y** is a rectangle of the space R3, which is defined as follows and has a hole ν.

$$Y=\left[0,Y_1\right]*\left[0,\ Y_2\right]*\left[0,Y_3\right] \tag{10}$$

The boundaries of ν are defined by *s* as follows:

$$\left(\partial\nu = s\right) \tag{11}$$

International Journal of Science and Engineering Applications
Volume 11-Issue 12, 254 – 265, 2022, ISSN:- 2319 - 7560
DOI: 10.7753/IJSEA1112.1002

It is assumed that it is smooth with sufficient size. In a general case, the traction *P* can also exist next to the hole. The solid part of the cell is defined by ¥ as follows:

$$\Omega_\varepsilon = \left\{ x \,\epsilon\, \Omega \mid \left(y = \frac{x}{\varepsilon} \right) \epsilon\, ¥ \right\} \tag{12}$$

The following relation is also defined:

$$S_\varepsilon = \bigcup_{i=1}^{Allcell} S_i \tag{13}$$

It is assumed that no hole ν_i crosses the boundary Γ.

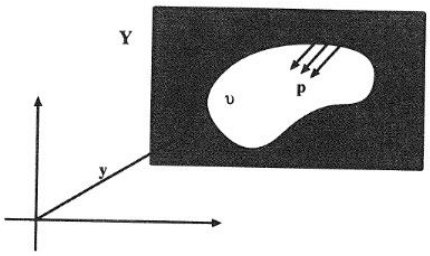

Figure 3. Cell body unit [26]

The followings are stress-strain and strain-displacement equations:

$$\sigma_{ij}^{\varepsilon} = E_{ijkl} e_{kl}^{\varepsilon}$$
$$\mathrm{e}_{kl}^{\varepsilon} = (\frac{1}{2})(\frac{\partial u_k^{\varepsilon}}{\partial x_l} + \frac{\partial u_l^{\varepsilon}}{\partial x_k}) \tag{14}$$

with condition $u^{\epsilon}\,\epsilon\, \nu^{\epsilon}$ the virtual displacement equation can also be defined as follows:

$$\int_\Omega E_{ijkl} \frac{\partial u_k^{\epsilon}}{\partial x_l} \frac{\partial \nu_i}{\partial x_j} d\Omega = \int_{\Omega^{\epsilon}} F_i^{\epsilon} \nu_i d\Omega + \int_{\Gamma_t} t_i \nu_i d\Gamma + \int_{s^{\epsilon}} P_i^{\epsilon} \nu_i dS \qquad \forall \nu\, \epsilon \nu^{\varepsilon} \tag{15}$$

by using the asymptotic expansion, Eq. (15) is expressed as follows:

$$\int_\Omega \mathrm{E}_{ijkl} \{ \frac{1}{\varepsilon^2} \frac{\partial \mathrm{u}_k^0}{\partial \mathrm{y}_l} \frac{\partial \mathrm{v}_i}{\partial \mathrm{y}_j} + \frac{1}{\varepsilon} \left[\left(\frac{\partial \mathrm{u}_k^0}{\partial \mathrm{x}_l} + \frac{\partial \mathrm{u}_k^1}{\partial \mathrm{y}_l} \right) \frac{\partial \mathrm{v}_i}{\partial \mathrm{y}_j} + \frac{\partial \mathrm{u}_k^0}{\partial \mathrm{y}_l} \frac{\partial \mathrm{v}_i}{\partial \mathrm{x}_j} \right] + \left[\left(\frac{\partial \mathrm{u}_k^0}{\partial \mathrm{x}_l} + \frac{\partial \mathrm{u}_k^1}{\partial \mathrm{y}_l} \right) \frac{\partial \mathrm{v}_i}{\partial \mathrm{x}_j} + \left(\frac{\partial \mathrm{u}_k^1}{\partial \mathrm{x}_l} + \frac{\partial \mathrm{u}_k^2}{\partial \mathrm{y}_l} \right) \frac{\partial \mathrm{v}_i}{\partial \mathrm{y}_j} \right] + \varepsilon(..) \} d\Omega =$$
$$\int_{\Omega^{\epsilon}} F_i \nu_i d\Omega + \int_{\Gamma_t} t_i \nu_i d\Gamma + \int_{s^{\epsilon}} P_i^{\epsilon} \nu_i dS \quad \forall \nu \epsilon \nu_{\Omega^* ¥} \tag{16}$$

Herein, by setting equal powers of ε and simplifying equations, the following equations are finally obtained. For further study, refer to reference [21].

$$\int_\Omega \left[\frac{1}{|Y|} \int_¥ \left(\mathrm{E}_{ijkl} - \mathrm{E}_{ijpq} \frac{\partial \chi_p^{kl}}{\partial \mathrm{y}_q} \right) \mathrm{dY} \right] \frac{\partial \mathrm{u}_k^0(\mathrm{x})}{\partial \mathrm{x}_l} \frac{\partial \mathrm{v}_i(\mathrm{x})}{\partial \mathrm{x}_j} d\Omega =$$
$$\int_\Omega \left(\frac{1}{|Y|} \int_¥ \mathrm{E}_{ijkl} \frac{\partial \Psi_k}{\partial \mathrm{y}_l} \mathrm{dY} \right) \frac{\partial \mathrm{v}_i(\mathrm{x})}{\partial \mathrm{x}_j} d\Omega + \tag{17}$$
$$\int_\Omega \left(\frac{1}{|Y|} \int_¥ \mathrm{f}_i \mathrm{dY} \right) \mathrm{v}_i(\mathrm{x}) d\Omega + \int_{\Gamma_t} \mathrm{t}_i \mathrm{v}_i(\mathrm{x}) d\Gamma \quad \forall \nu \epsilon \mathrm{V}_¥$$

to simplify the above equations, the following notations are considered:

$$E_{ijkl}^{\mathrm{H}}(\mathrm{x}) = \frac{1}{|Y|} \int_¥ \left(\mathrm{E}_{ijkl} - \mathrm{E}_{ijpq} \frac{\partial \chi_p^{kl}}{\partial \mathrm{y}_q} \right) \mathrm{dY}$$
$$\tau_{ij}(\mathrm{x}) = \int_¥ \mathrm{E}_{ijkl} \frac{\partial \Psi_k}{\partial \mathrm{y}_l} \mathrm{dY} \tag{18}$$
$$b_i(x) = \frac{1}{|Y|} \int_¥ \mathrm{f}_i \mathrm{dY}$$

Therefore, equation (16) can be written as follows:

$$\int_\Omega E_{ijkl}^{\mathrm{H}} \frac{\partial \mathrm{u}_k^0(\mathrm{x})}{\partial \mathrm{x}_l} \frac{\partial \mathrm{v}_i(\mathrm{x})}{\partial \mathrm{x}_j} d\Omega = \int_\Omega \tau_{ij}(\mathrm{x}) \frac{\partial \mathrm{v}_i(\mathrm{x})}{\partial \mathrm{x}_j} d\Omega +$$
$$\int_\Omega b_i(\mathrm{x}) \mathrm{v}_i(\mathrm{x}) d\Omega + \int_{\Gamma_t} \mathrm{t}_i \mathrm{v}_i(\mathrm{x}) d\Gamma \quad \forall \nu \epsilon \mathrm{V}_¥ \tag{19}$$

This Eq. (19) is very similar to virtual displacement Eq. (15) and shows the macroscopic balance. In the above equation, E_{ijkl}^H is the homogeneous elastic constant, τ_{ij} is the average stress remaining inside the cell, which is related to the traction *P* next to the hole, and b_i is the average volumetric force [21].

6. SOLVING EQUATIONS BY FINITE ELEMENT NUMERICAL METHOD

For the case where the thickness of the structure is small, (such as pipes and shells D>> t), the assumption of plane stress can be used for analysis, in this case, the stress and strain relationships become as follows:

$$\begin{Bmatrix} \sigma_1 \\ \sigma_2 \\ \tau_{12} \end{Bmatrix} = \begin{bmatrix} D_{11} & D_{12} & 0 \\ D_{12} & D_{22} & 0 \\ 0 & 0 & D_{66} \end{bmatrix} \begin{Bmatrix} \epsilon_1 \\ \epsilon_2 \\ \Upsilon_{12} \end{Bmatrix} \tag{20}$$

By using equation (19) and applying the simplifications and using the finite element method, the homogenized

elements of the matrix of elastic properties can finally be found. Interested readers are referred to reference [21].

$$D_{11}^H = \frac{1}{|Y|}\int_Y \left(D_{11} - d_1^T\ \epsilon(\psi)\right) dY$$
$$D_{12}^H = \frac{1}{|Y|}\int_Y \left(D_{12} - d_1^T \epsilon(\psi)\right) dY \qquad (21)$$
$$D_{22}^H = \frac{1}{|Y|}\int_Y \left(D_{22} - d_2^T \epsilon(\psi)\right) dY$$
$$D_{66}^H = \frac{1}{|Y|}\int_Y \left(D_{66} - d_3^T \epsilon(\psi)\right) dY$$

In the above relations ψ and $\epsilon(\psi)$ are the displacement field and the strain field respectively. d_1, d_2, d_3 are the columns of the elasticity matrix *D* and are defined as follows:

$$d_1 = \begin{Bmatrix} D_{11} \\ D_{12} \\ 0 \end{Bmatrix} \quad d_2 = \begin{Bmatrix} D_{12} \\ D_{22} \\ 0 \end{Bmatrix} \quad d_3 = \begin{Bmatrix} 0 \\ 0 \\ D_{66} \end{Bmatrix} \qquad (22)$$

Therefore, according to equation (21), homogenized elastic properties matrix elements can be obtained. For further reading, refer to reference [21].

7. FINITE ELEMENT SIMULATION

Here, Eq. (21) was solved using the finite element method, and the homogeneous modulus was obtained. Modeling of the single wall Carbon Nanotube is very sophisticated, therefore, in order to analyze and simulation of SWCNT, the model should be simplified. In this research, one of the impressed models which are presented is implemented [29]. The nanotube geometry was modeled by MATLAB software, which also was used by Ferdosi et al [30] to model single-walled carbon nanotubes to calculate the buckling and post-buckling behavior. In the homogeneous method, that are been used in this article, it is necessary to consider the cross-section of the carbon-carbon bond as a rectangle, Figure (6).

A space-frame model is here employed for the zigzag and armchair nanotubes with different chiralities and aspect ratios. In this approach, the linkage between carbon atoms is modeled as a three-dimensional elastic beam. By establishing a linkage between structural mechanics and molecular mechanics, the sectional property parameters of these beam members are obtained. The general potential energy, when the electrostatic interactions are ignored, is expressed as follows:

$$E = E_\rho + E_\theta + E_\omega + E_\tau + E_{VDW} + E_{EL} \qquad (23)$$

In the equation above, $E\rho$, E_θ, $E\omega$, and $E\tau$ are respectively the potentials related to bond stretching, angle changes, inversion, and twisting as shown in Figure (4). Also, E_{VDW} and E_{EL} are Vandals forces and electrostatic reactions, which both are caused by non-bonded reactions.

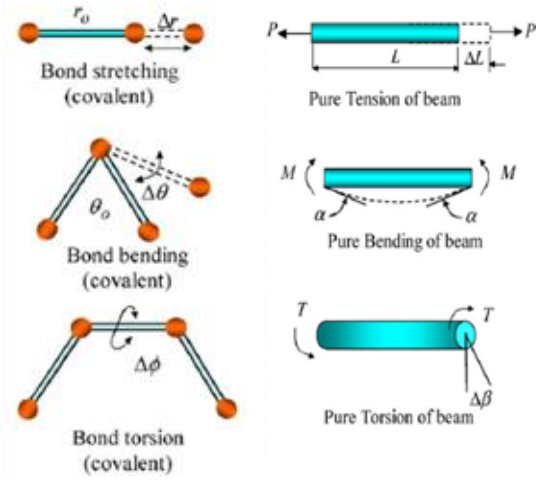

Figure 4. Interatomic reactions in molecular mechanics: (a) Tension. (b) Bending. (c) Inversion. (d) Torsion [27].

In single-walled carbon nanotubes, the first four terms that have the most effect are considered. The main energy distribution of all atoms comes from the first four terms of Eq. (23) and the potentials caused by non-bonded reactions can be ignored. Therefore, the energy of the system is expressed as follows:

$$E = E_\rho + E_\theta + E_\omega + E_\tau \qquad (24)$$

In the above equation, each of the terms is defined as follows:

$$E_\rho = \frac{1}{2}\sum_{Bonds} k_r(\Delta r_i)^2 \qquad (25)$$

$$E_\theta = \frac{1}{2}\sum_{angles} k_\theta(\Delta\theta_i)^2 \qquad (26)$$

$$E_\omega = \frac{1}{2}\sum_{Bonds} k_\omega(\Delta\omega_i)^2 \qquad (27)$$

$$E_\tau = \frac{1}{2}\sum_{Bonds} k_\tau(\Delta\phi_i)^2 \qquad (28)$$

And in the above relationship, Δri, $\Delta\Theta i$, $\Delta\omega i$, and $\Delta\varphi i$, respectively, show the bond stretching energy, bond angle bending energy, out-of-plane torsion energy, and dihedral

angle torsion energy. Moreover, *kr*, *kΘ*, *kω*, *kτ*, correspond to the force constants associated with the stretching, bending, and torsion of bonds. According to the structural mechanic's theory, the covalent forces between two carbon atoms are replaced by the 3D beam element and the carbon atoms act as the joint of the beam, which is shown in Figure (5).

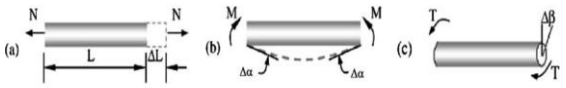

Figure 5. beam element: (a) Tension. (b) Bending. (c) Torsion [26].

Based on the theory of structural mechanics, the Calculation of strain energy for analysis of stress and strain, in different mechanical structures, is inevitable. Some structures should be analyzed for strength based on strain energy release to figure out the tolerance of the design under different loading conditions such as impact or quasi-static load [28]. Based on the theory of structural mechanics, the strain energy of a uniform beam under the axial force N, bending moment M, and torsion T is expressed as follows:

$$U_A = \frac{1}{2}\int_0^L \frac{N^2}{EA}dl = \frac{1}{2}\frac{N^2}{EA} = \frac{1}{2}\frac{EA}{L}(\Delta L)^2 \qquad (29)$$

$$U_M = \frac{1}{2}\int_0^L \frac{M^2}{EI}dl = \frac{1}{2}\frac{EI}{L}\alpha^2 = \frac{1}{2}\frac{EI}{L}(2\alpha)^2 \qquad (30)$$

$$U_T = \frac{1}{2}\int_0^L \frac{T^2}{GJ}dl = \frac{1}{2}\frac{T^2 L}{GJ} = \frac{1}{2}\frac{GJ}{L}(\Delta\beta)^2 \qquad (31)$$

In the above equations, *E* and *G*, are Young's modulus and shear modulus of the beam element, and *A*, *I*, *J*, and *L* respectively represent the cross-section, the moment of inertia, the polar moment of inertia, and the length of the beam element. In addition, ΔL, $\Delta\alpha$, and $\Delta\beta$ denote the deviation of bond length, bond angle, and dihedral angle from the equilibrium position, respectively. By comparing equations (25) to (28) with equations (29) to (30), the relationship between structural mechanic's parameters, *EA*, *EI*, and *GJ*, with molecular mechanic's parameters, *kr*, k_θ, and $k\tau$ will be established as follows:

$$\frac{EA}{L} = k_r \qquad (32)$$

$$\frac{EI}{L} = k_\theta \qquad (33)$$

$$\frac{GJ}{L} = k_\tau \qquad (34)$$

Herein, the force coefficients *kr*, *kΘ*, and $k\tau$ are known as hardness constants. The values are presented in table (1).

Table 1. Values used for force constants [26].

k_r	k_θ	k_τ
6/52*7-10 *N/nm*	8/76*7-10 *N nm/rad²*	2/78*7-10 *N nm/rad²*

According to Eqs. (32-34), *EA*, *EI*, and *GJ* can be gained by choosing the appropriate cross-section. By choosing a rectangular cross section for the carbon-carbon bond, which is shown in Figure (6), the desired properties for the written code are obtained.

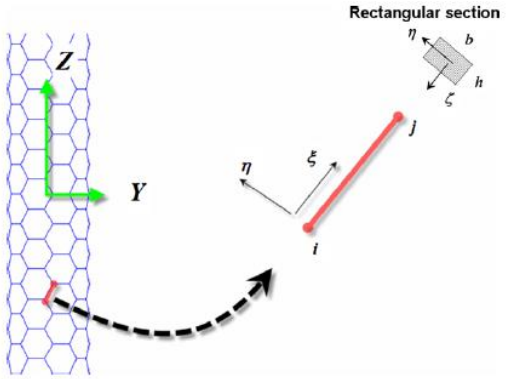

Figure 6. rectangular cross section for carbon-carbon bond [26].

For the rectangular cross section, the area and moment of inertia will be achieved from the following equations:

$$A = bh \quad I_{\xi\xi} = \frac{b^3 h}{12} \quad I_{\eta\eta} = \frac{bh^3}{12} \quad J = I_{\xi\xi} + I_{\eta\eta} \qquad (35)$$

Then, by comparing equations (32) and (33), the following formula for parameter *b* will be obtained.

$$b = \sqrt{12\frac{k_\theta}{k_r}} \qquad (36)$$

By substitution force coefficient values presented in table (3) on Eq. (36) the value of 0.127 nm will be obtained for parameter *b*. The rest of the parameters consist of Young's modulus (*E*), shear modulus (*G*), and Poisson's ratio (υ) are also obtained from the aforementioned equations. The values used in this article are presented in Table (2). In this article, the *h* parameter is taken as the thickness parameter of the nanotube and is equal to 0.34 nm.

International Journal of Science and Engineering Applications
Volume 11-Issue 12, 254 – 265, 2022, ISSN:- 2319 - 7560
DOI: 10.7753/IJSEA1112.1002

Table 2. Information entered for single-walled nanotubes from the article [26].

E	*G*	υ	*b*	*h*
2.144 (TPa)	0.825 (TPa)	0.3	0.127 (nm)	0.34 (nm)

Therefore, by entering the information presented in table (2), the matrix of elastic properties for the desired unit cell shown in figure (7) was calculated. Obtained results for armchair and zigzag nanotubes are reported in tables (3) and (4).

Table 3. The results for the elastic properties matrix of 1050 4-node elements for armchair (Terapascal units).

D_{11}	D_{12}	D_{22}	D_{66}
1.098	0.361	0.993	0.352

Table 4. The results for the elastic properties matrix of 1050 4-node elements for zigzag (Terapascal units).

D_{11}	D_{12}	D_{22}	D_{66}
0.997	0.360	1.105	0.349

By assuming the plane stress state and for an orthotropic material, the relationship between the matrix coefficients of elastic properties and the mechanical properties are defined as bellow:

$$D_{11}=\frac{E_1}{1-\nu_{12}\nu_{21}} \quad D_{21}=\frac{\nu_{12}E_1}{1-\nu_{12}\nu_{21}} \qquad (37)$$
$$D_{22}=\frac{E_2}{1-\nu_{12}\nu_{21}} \quad D_{66}=G_{12}$$

Since the matrix of elastic properties is symmetry, it is concluded that:

$$\frac{\nu_{12}}{E_1}=\frac{\nu_{21}}{E_2} \qquad (38)$$

There are five equations and five unknowns in this. The mechanical characteristics of zigzag and armchair nanotubes are concurrently determined by solving these equations.

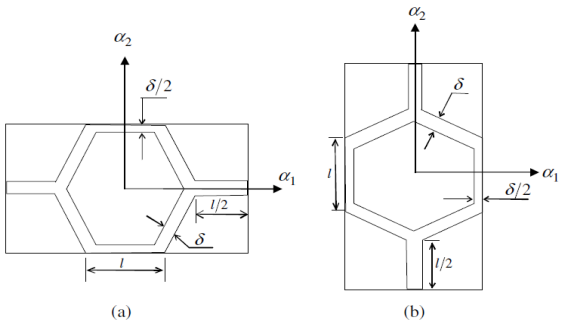

Figure 7. carbon nanotube unit cell (a) armchair (b) zigzag [14].

8. DISCUSSION AND CONCLUSION

This study used the asymptotic homogenization method to examine the mechanical properties of single-walled carbon nanotubes for zigzag and armchair nanotubes. Here, just the Wander wall forces are taken into account in a periodic arrangement of single-walled carbon nanotube unit cells. In actuality, the homogenization procedure substituted the intended structure for an equivalent homogenized model that behaved identically to the initial heterogeneous structure.

The homogenized equations are resolved using the finite element method. For a wall thickness of 0.34 nm, the information needed to be taken from the article [26] was altered, and the issue was resolved for 1050 4-node elements. Tables (3) and (4) for armchair and zigzag nanotubes, respectively, show the obtained results. The armchair's Young's modulus and the zigzag nanotube's shear modulus were determined by using the values shown in Tables (3) and (4) and using equations (37) and (38). Young's modulus results are illustrated in Figures (8-10) and contrasted with results from various articles.

A. Young's modulus: Figures (8-10) show Young's modulus for armchair and zigzag nanotubes that were obtained using the homogenization method.

The amount of Young's modulus achieved for the zigzag and armchair nanotubes is 0.972 TPa and 0.875 TPa, respectively, as illustrated in Figure (8). It is evident that the zigzag Young's module is larger than the armchair. According to Li and Chou [10], Kalamkarov et al. [14], and Rafiee et al. [16], the mechanical properties of carbon nanotube cells are affected by their orientation, which accounts for this variation. The Young's module zigzag in Figure (8) is almost 8% larger than the armchair, which is reasonably close to the outcomes reported by Sao et al. [13]. They discovered a 5% variation in modulus between

International Journal of Science and Engineering Applications
Volume 11-Issue 12, 254 – 265, 2022, ISSN:- 2319 - 7560
DOI: 10.7753/IJSEA1112.1002

zigzag and armchair. Arroyo et al. [9] also predicted the same values for Young's modulus of the armchair and zigzag nanotubes in large diameters.

The Young's modulus for carbon nanotubes acquired using the current method for various diameters yields the same values, as can be seen from Figures (9) and (10), which is in good agreement with the outcomes obtained using the homogenization method of Kalamkarov et al. [14]. The Young's modulus values achieved at small diameters vary from those obtained using other methods. As shown in Figures (9) and (10), Rafiee et al. [16], Xiao et al. [13], Arroyo et al. [9], and Li and Chou [10] indicated that Young's modulus of both armchair and zigzag nanotubes will increase at low diameters with increasing diameters of the nanotube. Also, it is shown that in the larger diameters the growth in Young's modulus magnitude stops and reaches a constant level.

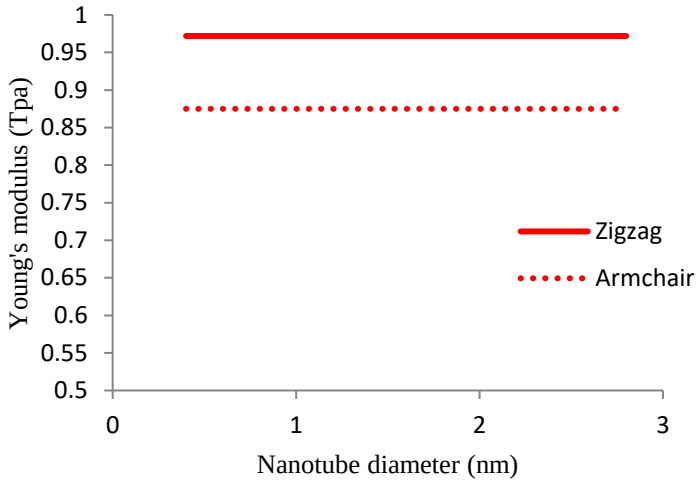

Figure 8. Comparison of the obtained results for Young's modulus of armchair and zigzag nanotubes from homogenization method.

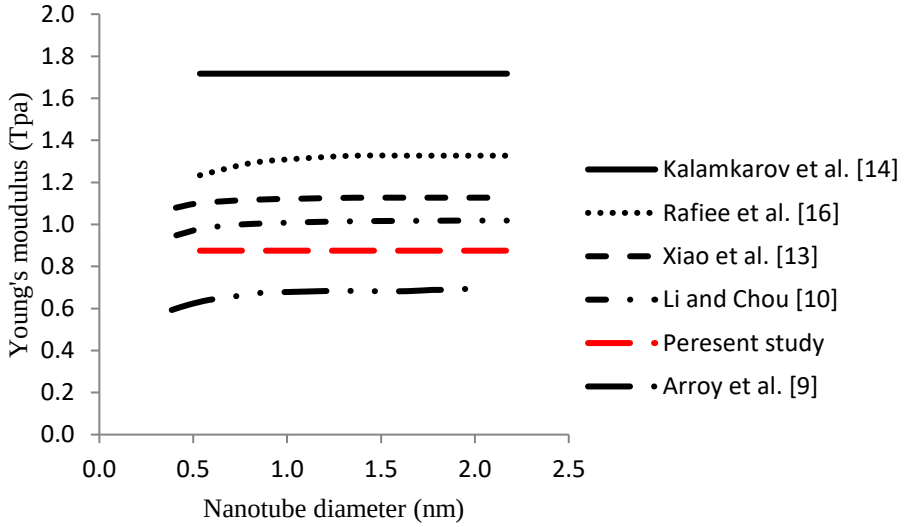

Figure 9. Comparison of the present obtained results for the Young's modulus of the armchair with different articles.

The homogenization method's formulation ignores the influence of the nanotube's curvature, which is the cause of these minor variations in smaller diameters. In fact, the carbon-carbon bonds are more distorted at lower diameters because the nanotube has higher curvature at smaller diameters. The impact of bond distortion and curvature steadily diminishes as the diameter of the nanotubes grows. Because of this, the influence of diameter and curvature on mechanical qualities in larger diameters is much diminished. The current findings produced by the homogenization approach obtained results from other different described ways as a result of increasing the diameter.

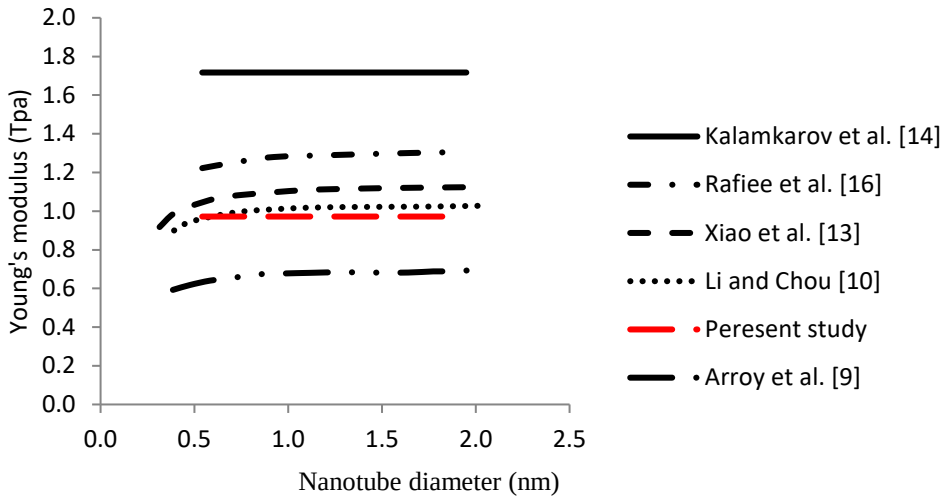

Figure 10. Comparison of the present obtained results for the Young's modulus of zigzag with different articles.

B. Shear modulus: Figures (11-13) show the shear modulus for armchair and zigzag nanotubes that were obtained using the homogenization method.

As it is shown in Figures (11-13), the shear modulus for the armchair and zigzag nanotubes are, consequently, 0.352 TPa and 0.349 TPa, which are in suitable assent with the gained results by Chandraseker and Mukherjee [15], and also Li and Chu. [10]. Kalamkarov et al. [14], predicted the difference between magnitude of the shear modulus of armchair and zigzag nanotubes. In Figure (11), the shear module armchair is about 2.4% larger than zigzag, which is acceptably close to the results declared by Kalamkarov et al. [14]. As can be seen in Figures 12 and 13, the prediction of the values obtained for the shear modulus in armchair and zigzag nanotubes are in good agreement with the predictions obtained by the Figures method of Kalamkarov et al [14], and Chandraseker et al [15]. Moreover, it is illustrated that the small differences in lower diameters, which are also mentioned in the previous part, exist in the shear module too. The amount of distinction is reduced by increasing the diameter.

International Journal of Science and Engineering Applications
Volume 11-Issue 12, 254 – 265, 2022, ISSN:- 2319 - 7560
DOI: 10.7753/IJSEA1112.1002

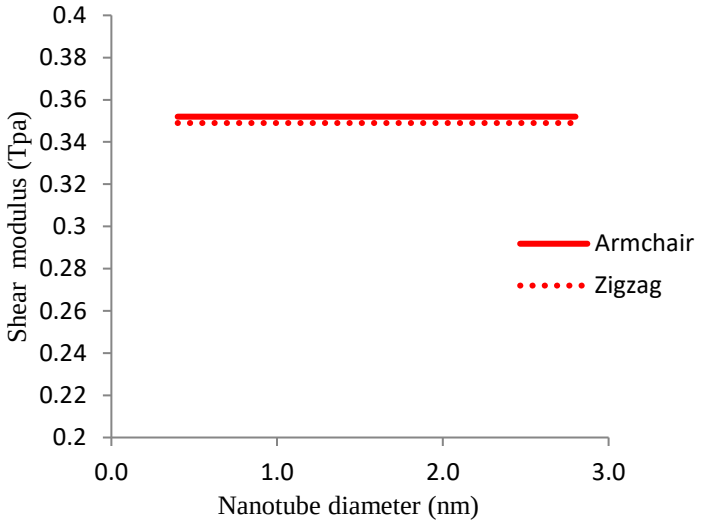

Figure 11. Comparison of the obtained results for shear modulus of armchair and zigzag nanotubes from homogenization method.

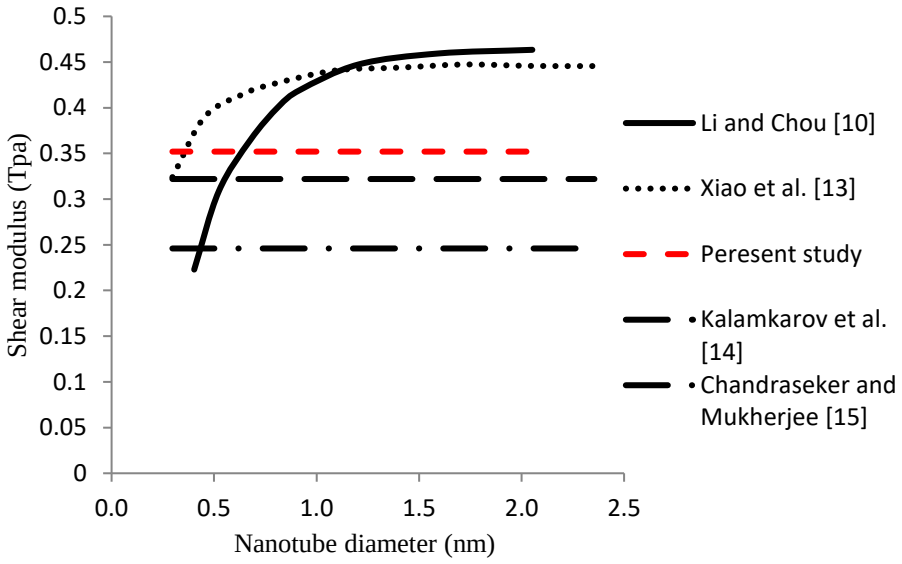

Figure 12. Comparison of the present obtained results for the shear modulus of armchair with different articles.

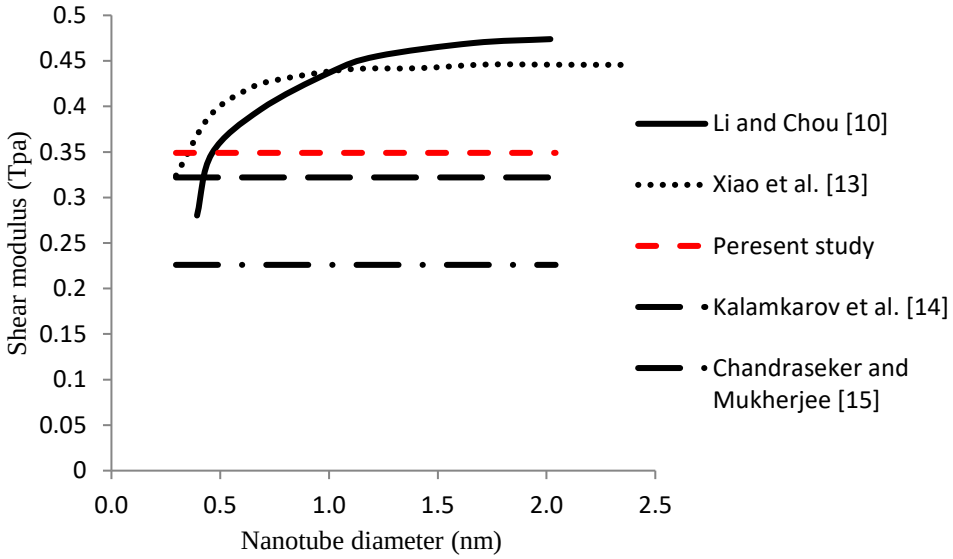

Figure 13. Comparison of the present obtained results for the shear modulus of zigzag with different articles.

As shown in Figures (8-10) for Young's modulus and Figures (11-13) for shear modulus, the results obtained from the homogenization method are in good acceptance with the gained results from different articles. The differences in the results in distinct articles can be considered as a result of the different parameters and methods used in predicting the mechanical properties of carbon nanotubes like the wall thickness and Carbon-Carbon cross-section area.

One of the advantages of homogenization method is the less computational effort in predicting the mechanical properties of nanotubes compared to other methods. By measuring the homogenized elastic coefficients, the hexagonal atomic model can be replaced with the homogeneous model of nanotubes. Hence, we will be able to find all the properties and requirements of nanotubes such as free vibrations, buckling, bending, etc.

9. CONCLUSION

In this study, the asymptotic homogenization approach was used to calculate the Young's and shear modulus of single-walled carbon nanotubes for armchair and zigzag nanotubes. 1050 4-node elements were employed in the finite element method to solve the obtained equations. Although Young's modulus and shear modulus values of carbon nanotubes calculated using this method are not sensitive to variations in diameter, the results demonstrate that different outcomes can be achieved by altering the orientation of carbon nanotubes. Young's modulus of carbon nanotubes for the armchair and zigzag nanotubes is calculated using the asymptotic homogenization approach to be 0.875 and 0.972 TPa, respectively. Likewise, the shear modulus is 0.352 TPa for one and 0.349 TPa for the other. Both of these have strong concordance with other approaches discussed in earlier studies.

10. REFERENCES

[1] Kroto HW, Heath JR, O'Brien SC, Curl RF, Smalley RE. 1985. "C60: Buckminsterfullerene". Nature 318:162–3.
[2] S.Iijima. 1991. "Helical microtubules of graphitic carbon". Nature 354 (1991) 56.
[3] Collins PG, Avouris P. 2000. "Nanotubes for electronics". Scientific American 283(6):67–69.
[4] Mintmire JW, Dunlap BI, White CT. 1992. "Are fullerene tubules metallic". Physics Review Letters 68:631–634.
[5] Krishnan A, Dujardin E, Ebbesen TW, Yianilos PN, Treacy MMJ. 1998. "Young's modulus of single-walled nanotubes". Phys Rev B 58;14013–9.
[6] Tombler TW, Zhou CW, Alexaeyev L, Kong J, Dai HJ, Liu L, et al. 2000. "Reversible electromechanical characteristics of carbon nanotubes under local-probe manipulation". Nature 405:769–72.
[7] Salvetat JP, Briggs GAD, Bonard JM, Bacsa RR, Kulik AJ, Stockli T, et al. 1999. "Elastic and shear moduli of single-walled carbon nanotube ropes". Phys Rev Lett 82(5):944–7.
[8] Hernandez E, Goze C, Bernier P, Rubio A. 1998. "Elastic properties of C and BxCyNz composite nanotubes". Phys Rev Lett 80(20):4502–5.
[9] Arroyo M, Belytschko T. 2002. "Large deformation atomistic-based continuum analysis of carbon nanotubes". American Institute of Aeronautics and Astronautics b;1–10.
[10] Li C, Chou TWA. 2003. "Structural mechanics approach for the analysis of carbon nanotubes". Int J Solid Struct 40:2487–99.
[11] Jin Y, Yuan FG. 2003. "Simulation of elastic properties of single-walled carbon nanotubes". Compos Sci Techno 63(11):1507–15.
[12] Tserpes KI, Papanikos P. 2005. "Finite element modeling of single-walled carbon nanotubes". Compos: Part B Eng 36(5):468–77.
[13] Xiao JR, Gama BA, Gillespie Jr JW. 2005. "An analytical molecular structural mechanics model for the

mechanical properties of carbon nanotubes". Int J Solids Struct 42:3075–92.
[14] Kalamkarov AL, Georgiades AV, Rokkam SK, Veedu VP, Ghasemi-Nejhad MN. 2006. "Analytical and numerical techniques to predict carbon nanotubes properties". Int J Solid Struct 43:6832–54
[15] Chandraseker K, Mukherjee S. 2006. "Atomistic-continuum and ab initio estimation of the elastic moduli of single-walled carbon nanotubes". Computational Materials Science 40:147–158.
[16] Rafiee R, Heidarhaei M. 2012. "Investigation of chirality and diameter effects on Young's modulus of carbon nanotubes using non-linear potentials". Composite Structures 94:2460–2464.
[17] Xiaoxing Lu, Zhong Hu. 2012. "Mechanical property evaluation of single-walled carbon nanotubes by finite element modeling". Composites Part B 43:1902–1913.
[18] Dresselhaus MS, Dresselhaus G, Saito R. 1995. "Physics of carbon nanotubes". Carbon 33(7):883–91.
[19] Thostenson ET, Ren Z, Chou TW. 2001. "Advances in the science and technology of carbon nanotubes and their composites: a review". Composites Science and Technology 61:1899–1912.
[20] Dresselhaus MS, Dresselhaus G, Eklund PC, editors. 1996. "Science of fullerenes and carbon nanotubes". New York: Academic Press.
[21] Hassani B, Hinton E. 1999. "Homogenization and structural topology optimization". New York: Springer.
[22] Sanchez-Palencia E. 1980. "Non-homogenous media and vibration theory". LectureNotes in Physics 127.
[23] Benssousan A, Lions J, Papanicoulau G. 1987. "Asymptotic analysis for periodic structures". North-Holland: Amsterdam.
[24] Cioranescu D, Paulin JSJ. 1979. "Homogenization in open sets with holes". Journal of Math, Analysis and Appl 71: 590-607.
[25] Guedes JM, Kikuchi N. 1990. "Pre and post processing for materials based on the homogenization method with adaptive finite element methods". Compo Meth Appl Mech Eng 83:143-198.
[26] Wan H, DelaleA F. 2010. "Structural mechanics approach for predicting the mechanical properties of carbon nanotubes". Meccanica 45:43-51.
[27] R. Ansari, S.Rouhi. 2010. "Atomistic finite element model for axial buckling of single-walled carbon nanotubes". Physica E43(2010)58–69.
[28] M.R.Gharib, M.Rasti, P.Danesha, R.Daneshvar, N.Mohammadyahya,. 2022. "Analysis of stress and strain of human skull bone in physical injury" Mechanics of Solids. https://doi.org/10.3103/S0025654422050065.

[29] S.B.Ferdosi, N.Mohammadyahya, M.Abasi. 2022. "Axial Buckling of Single-walled Nanotubes Simulated by an Atomistic Finite Element Model under Different Temperatures and Boundary Conditions". International Journal of Science and Engineering Applications. Volume 11-Issue 11, 151-163, 2022, ISSN: -2319-7560. DOI: 10.7753/IJSEA1111.1002.
[30] S.B.Ferdosi, B.Hassani, A.Daneshvar. 2015. "Numerical simulation of buckling and postbuckling of single-wall carbon nanotubes". JSFM_Volume 5_Issue 1_Pages 77-86.